Smart Structures and Systems, *Vol. 22, No. 6 (2018) 663-673*
DOI: https://doi.org/10.12989/sss.2018.22.6.663

The effect of particle size on the edge notched disk (END) using particle flow code in three dimension

Hadi Haeri[1], Vahab Sarfarazi[2], Zheming Zhu*[1] and Mohammad Fatehi Marji[3]

[1]MOE Key Laboratory of Deep Underground Scienceand Engineering,
School of Architectureand Environment, Sichuan University,Chengdu 610065, China
[2]Department of Mining Engineering, Hamedan University of Technology, Hamedan, Iran
[3]Department of Mining Engineering, Yazd University, Yazd, Iran

(Received August 18, 2018, Revised November 27, 2018, Accepted November 29, 2018)

Abstract. In this study, the effect of particle size on the cracks propagation and coalescence or cracking pattern of the edge notched disc specimens are investigated. Firstly, calibration of PFC3D was performed using Brazilian experimental test output. Then micro parameters were used to build edge notched disc specimen. The horizontal wall of the assembly is let to move downward with a standard low speed of 0.016 m/s. The numerical results show that the tensile cracks are dominant failure pattern for the modeled discs. These tensile cracks initiate from the pre-existing notch tip and propagate parallel to the loading direction then interact with the upper boundary of the modeled specimen. As the size of the balls (ball diameter) decrease the number of tensile cracks increase. The tensile fracture toughness of the samples also decreases as the particle size increases. Understanding the crack propagation and crack coalescence phenomena in brittle materials such as concretes and rocks is of paramount importance in the stability analyses for engineering structures such as rock slopes, underground structures and tunneling.

Keywords: END test; pre-existing edge crack; PFC3D

1. Introduction

In rock engineering the fracture mechanics principles are of importance in most problems related to the strength and stress analyses in rocks. The fundamental of rock fracture mechanics may help to establish a reasonable relationship between the fracturing strength and the geometry of cracks within the rock masses existed in different rock engineering projects. Thus, the fracture mechanics parameters such as the fracture toughness and the geometry of cracks should be determined because they can describe the resistance of rock materials to cracks initiation, propagation and coalescence. However, it is concluded that for quasi-brittle geo-materials such as concretes, the crack propagation phenomenon and the crack growth pattern are the main reasons for the final failure of these materials under different practical loading conditions. Therefore, investigations and understanding the fracturing mechanism and behavior of geo-materials are important in many rocks engineering process such as rock fragmentation by blasting or by rock cutting tools or in the stability analyses of underground and surface rock structures. Most of the numerical and experimental investigations can be validated through the theoretical studies (Wu *et al.* 2010, Lancaster *et al.* 2013, Ramadoss 2013, Pan *et al.* 2014, Mobasher *et al.* 2014, Noel and Soudki 2014, Oliveira and Leonel 2014, Kim and Taha 2014, Tiang *et al.* 2015, Wan Ibrahim *et al.* 2015, Lee and Chang 2015, Kequan and Zhoudao 2015, Silva *et al.* 2015, Gerges *et al.* 2015, Liu *et al.* 2015, Wasantha *et al.* 2015, Fan *et al.* 2016, Li *et al.*, 2015, 2016, Sardemir 2016, Sarfarazi *et al.* 2016, Shuraim 2016, Wang *et al.* 2016, 2017, Akbas 2016, Rajabi 2016, Mohammad 2016, Yaylac 2016, Najigivi *et al.* 2017a,b; Khodayar and Nejati 2018).

Because of its paramount importance several important methods have been suggested to determine the Mode I (opening or tensile mode) fracture (SCB) toughness of rocks. These methods include the Chevron Bend (CB) specimens, the Notched Brazilian Disc (NBD) type specimens, the Semicircular Bend (SCB) specimens, the Hollow Center Cracked Disc (HCCD) specimens, the Short Rod (SR) type specimens, the Hollow Center Cracked Disc Edge-Notched Round Bar In Bending (HCCD-ENRBB) specimens, The Hollow Center Cracked Quadratic Samples (HCCQS), the Edge-Notched Disc (END) type specimens and the Compact Tension (CT) tests (Barker 1977, Ouchterlony 1980, Atkinson 1982, Shiryaev and Kotkis 1982, Chong and Kuruppu 1984, Huang 1985, Ouchterlony 1986, BanksSills 1986, Buchholz 1987, Chong 1987, Ouchterlony 1988, Mahajan 1989, Maccagno 1989, He 1990, Suresh 1990, Singh 1990, Karfakis and Akram 1993, Lim et al. 1993, 1994, Khan 2000, Molenar *et al.* 2002, Chang 2002, Sato 2006, Obara *et al.* 2007, 2009, 2010, ISRM 2007, Dai *et al.* 2010, Kataoka 2011, Tutluoglu 2011, Amrollahi *et al.* 2011, Aliha *et al.* 2015a, b, Zhou *et al.* 2012, Kataoka 2012, 2013, Ramadoss 2013, Ayatollahi and Alborzi 2013, Kuruppu *et al.* 2014, Pan 2014, Kequan

*Corresponding author, Professor
E-mail: zhemingzhu@hotmail.com

http://www.techno-press.com/journals/sss&subpage=7 ISSN: 1738-1584 (Print), 1738-1991 (Online)

2015, Lee 2015, Akbas 2016, Rajabi 2016, Sarfarazi *et al.* 2014, Haeri *et al.* 2014, Haeri *et al*. 2015a, b, c, d, e, f, Sarfarazi *et al.* 2016a, b, c, Sarfarazi and Haeri *et al*. 2016, Haeri and Sarfarazi 2016a, Haeri *et al.* 2016b, Mohammad 2016, Fayed 2017).

The previous results show that an analysis of the stress distribution around a crack indicates the points of fracture initiation as well as the initial direction of crack propagation. As a result of the change in stress distribution associated with fracture propagation it is, however, impossible to predict the final path of the propagating crack. Consequently, a serious limitation of the Griffith theory lies in the fact that it can only be used to predict fracture initiation. In its usual form, it yields no information on the rate or direction of fracture propagation. The earlier studies have shown that two kinds of cracks, e.g., wing cracks and secondary cracks, may initiate from the tip of a single open crack under uniaxial compression. Wing cracks are induced by the tensile force, while secondary cracks are the result of shear force. In the loading process, wing cracks appear earlier than secondary cracks. The secondary cracks make the failure of the whole specimen. Sarfarazi (2014), tensile wing cracks were found to first appear at the tips of horizontal joints, followed by the secondary shear cracks propagating towards the opposite joint. Haeri (2014) represent that under internal or external pressures, pre-existing defects can induce macro crack, which can in turn change the structure of the rock.

Fayed (2017) represent that presence of natural weaknesses around the crack tip could change the stress distribution around the crack tip and lead to variations of characteristics of crack tip plastic zone such as plastic zone size and plastic zone shape. Such micro defects affect the fracture toughness and extension or kinking of the macro crack. Haeri *et al*. (2016b) represent that when cracks are analyzed, the behavior of the material ahead of the crack tip is considered isotropic, i.e., plastic deformation occurs identically in all directions and there are no preferred directions for the plastic deformation. In this case, the plastic deformation can be mathematically formulated with the help of classical isotropic plasticity. This situation significantly differs when the crack tip is near a micro-defect; the plastic zone ahead of the crack tip will be affected by the presence of the micro-defects.

Theoretically, linear elastic stress analysis of cracks predicts infinite stresses at the crack tip. In fact, inelastic deformation, such as plasticity in ductile and brittle materials, leads to relaxation of crack tip stresses caused by the yielding phenomenon at the crack tip (Mohammad 2016).

Khan (2000) represent that most rock materials develop plastic strains when the yield strength is exceeded in the region near a crack tip. Thus, the amount of plastic deformation is restricted by the surrounding material, which remains elastic during loading. The formation of the plastic zone in a homogeneous material depends on the material properties, structural element configuration, and loading conditions. The size of the plastic zone can be estimated when moderate crack tip yielding occurs.

In the present study the End-Notched Disc (END) type specimens are used to study the crack initiation and propagation mechanism in solid brittle materials.

Fig. 1 shows the Schematic view and dimensions of End type specimens used in this study (Isida 1979). END type specimen includes a disc of dimensions 2.75 cm both in diameter (D) and thickness (B). At the surface of the disc a straight edge crack with a varying length of "*a*" is created. The Mode *I* fracture toughness of END specimen can be obtained from

$$KIC = F(P/D)\sqrt{(\pi a)} \tag{1}$$

Where *P* is applied compression load and *F* is non-dimensional stress intensity factor. *YI* is depend on *a* and *D* and range from 0.1 to 0.6 (Table 1).

However, in this study, the crack propagation mechanism of concrete specimens is investigated by simulating some edge notched disk test through a 3D discrete element approach using a sophisticated particle flow code (PFC3D)). The crack initiation and propagation of the preexisting internal cracks is investigated by simulating the edge notched disk test. The effects of cracks particle size on the specimens fracturing path with in the bridge areas of the samples are studied by this numerical simulation procedure.

2. Numerical simulation

2.1 Bonded particle model and Particle Flow Code 3D (PFC3D)

Potyondy and Cundall (2004) developed a three dimensional discrete element code known as Particle flow code in three dimensions (PFC3D) based on the original code produced by Itasca 1999 version 3.1.

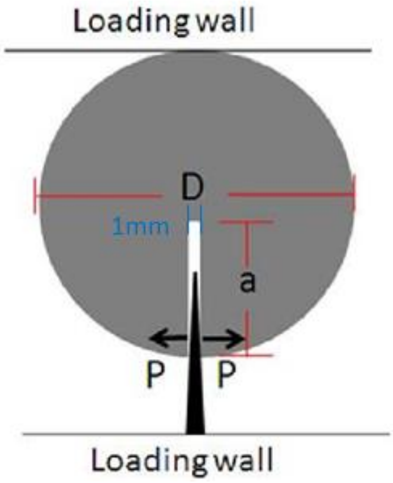

Fig. 1 Edge notched disk specimen and loading geometry

Table 1 Values of a=D and corresponding value of YI from Isida *et al*. (1979)

a/D	0.1	0.2	0.3	0.4	0.5	0.6
F	11.48	7.72	7.05	7.45	8.63	10.99

Table 2 Micro properties used to represent the intact rock

Parameter	Value	Parameter	Value
Type of particle	disc	Parallel bond radius multiplier	1
density	3000	Young modulus of parallel bond (GPa)	40
Minimum radius	0.27	Parallel bond stiffness ratio	1.7
Size ratio	1.56	Particle friction coefficient	0.4
Porosity ratio	0.08	Parallel bond normal strength, mean (MPa)	70
Damping coefficient	0.7	Parallel bond normal strength, SD (MPa)	2
Contact young modulus (GPa)	40	Parallel bond shear strength, mean (MPa)	70
Stiffness ratio	1.7	Parallel bond shear strength, SD (MPa)	2

Table 3 Brazilian tensile strength of physical and numerical samples

Physical tensile strength (MPa)	4.5 and 4.7
Numerical tensile strength (MPa)	4.5

This sophisticated DEM numerical code simulate the material samples as an assembly of rigid individual particles then, based on the central finite difference algorithm and calculate the interaction forces in between the particles and their relative movements from one another. The contacts within the particle assembly are modeled by both linear and non-linear contact models considering the frictional sliding that may occur at these contact points.

In this study, the linear contact model is used to provide an elastic relationship between the contact forces and the corresponding relative displacements of the particles. Based on the routines suggested by Itasca code 1999 version 3.1, a parallel bond particle model is generated for PFC3D and the following micro properties are defined to model a particular particle assembly: the contact modulus for ball-to-ball, the stiffness ratio Kn over Ks, the friction coefficient of ball. The parallel normal and shear bonding strengths, ratio of bonding strength standard deviation to that of the mean strength both in normal and shear directions at the contact points, the minimum ball radius, the multiplier of the parallel-bond radius, the modulus and stiffness ratio of parallel bond.

The appropriate micro properties for the particle assembly are stablished based on a standard calibration process adopted in PFC3D. However, the particle bonding characteristics and its contact properties cannot be directly determined from the macro properties gained due to the performance of some laboratory tests on the standard material samples. The macro mechanical properties obtained from the real material testing can be used as a basis for the calibration of the numerical procedure and select the appropriate micro mechanical properties for the modelled particle assembly which can be used to simulate the geo-mechanical engineering problems. The computer code provided by Itasca (1999), involves a trail-an-error approach to relate these two sets of material properties.

In this Algorithm, the micro mechanical properties are assumed at the beginning and the macro mechanical properties corresponding to them are approximately determined then this procedure is repeated so that the suitable micro mechanical properties for the particle assembly are determined where the corresponding macro mechanical properties (such as deformation and strength) get very close to those of laboratory testing results. The numerical model can be calibrated by comparing these two sets of results for the Brazilian tensile test.

2.2 Preparing and calibrating the numerical model

The calibration process of the PFC3D can be accomplished by using the Brazilian tensile strength of the material specimens and generate a particular particle assembly model. This standard procedure may involve the following four steps: i) generation and packing of the particles, ii) installation of isotropic stress condition within the particle assembly, iii) elimination of floating particles and iv) installation of particle bonding scheme. Based on these steps and adopting the micro-properties given in Table 2, the standard calibration procedures proposed by Potyondy and Cundall (2003) can used to obtain a standard calibrated particle assembly model for PFC3D. In this calibration process, the Brazilian tensile test is considered and the Brazilian discs with 54 mm diameter and 15615 particles within the modeled particle assembly are used. The lateral walls of the assembly are let to move toward one another with a standard low speed of 0.016 m/s. The failure patterns obtained from the numerical and experimental testing samples are illustrated in Figs. 2(a) and 2(b), respectively for comparison. These Figures show that the corresponding numerical and experimental failure patterns are well matching. Table 3 also compares the numerical and experimental values of the tensile strengths of the specimens which are in good agreement with each other. Therefore, the calibration procedure is succeeded and therefore, the edge notched Brazilian disc specimens can be numerically simulated by PFC3D to study the crack initiation and propagation of the pre-cracked discs.

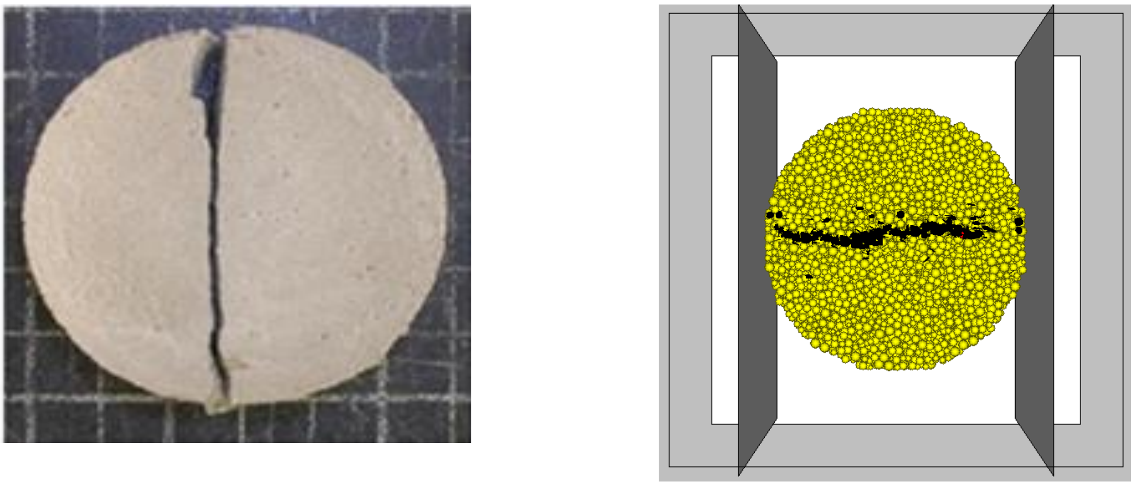

Fig. 2 failure pattern in (a) physical sample and (b) PFC2D model

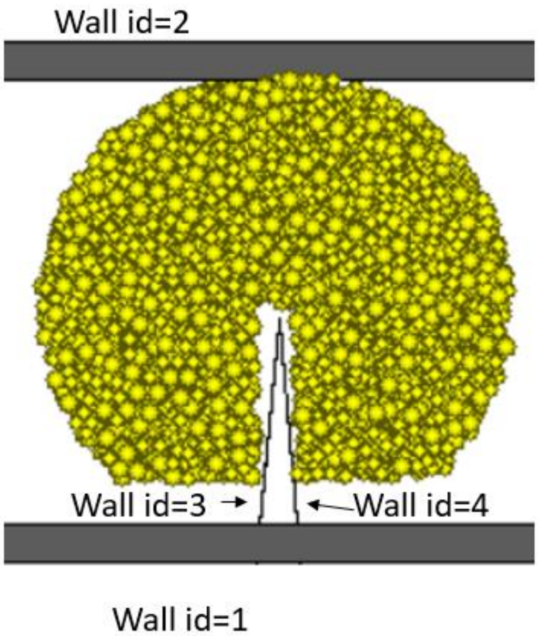

Fig. 3 Edge notched disk model in PFC3D

2.3 model preparation using Particle Flow Code

After calibration of PFC3D, edge notched disk test were simulated by creating a circle model in PFC2D (by using the calibrated micro-parameters) (Fig. 3). The PFC specimen had diameter of 54 mm and thickness of 27 mm. minimum diameter of balls changes in 18 different values i.e., 0.95 mm (Fig. 4(a)), 1.05 mm (Fig. 4(b)), 1.15 mm (Fig. 4(c)), 1.25 mm (Fig. 4(d)), 1.35 mm (Fig. 4(e)), 1.45 mm (Fig 4(f)), 1.55 mm (Fig. 4(g)), 1.65 mm (Fig. 4(h)), 1.75 mm (Fig. 4(i)), 1.85 mm (Fig. 4(j)), 1.95 mm (Fig. 4(k)), 2.05 mm (Fig. 4(l)), 2.15 mm (Fig. 4(m)), 2.25 mm (Fig. 4(n)), 2.35 mm (Fig. 4(o)), 2.45 mm (Fig. 4(p)), 2.55 mm (Fig. 4(q)), 2.65 mm (Fig. 4(r)), 2.75 mm (Fig. 4(s)), 2.85 mm (Fig. 4(t)) and 2.95 mm (Fig. 4(u)). Totally, 21 models consisting various ball number has been built, i.e., 31283 balls, 25252 balls, 19751 balls, 15380 balls, 12209 balls, 9853 balls, 8066 balls, 6687 balls, 5605 balls, 4744 balls, 4051 balls, 3486 balls, 3022 balls, 2637 balls, 2314 balls, 2042 balls, 1811 balls, 1614 balls, 1444 balls, 1297 balls and 1170 balls. These models are loaded by four loading walls (Fig. 3). The Tensile force was registered by taking the reaction forces on the wall id=1 (Fig. 3).

3. Numerical results

3.1 The effect of particle size on the failure pattern of specimens

Figs. 5(a)-5(u) shows the effect of particle size on the failure pattern of models with number of balls of 55343

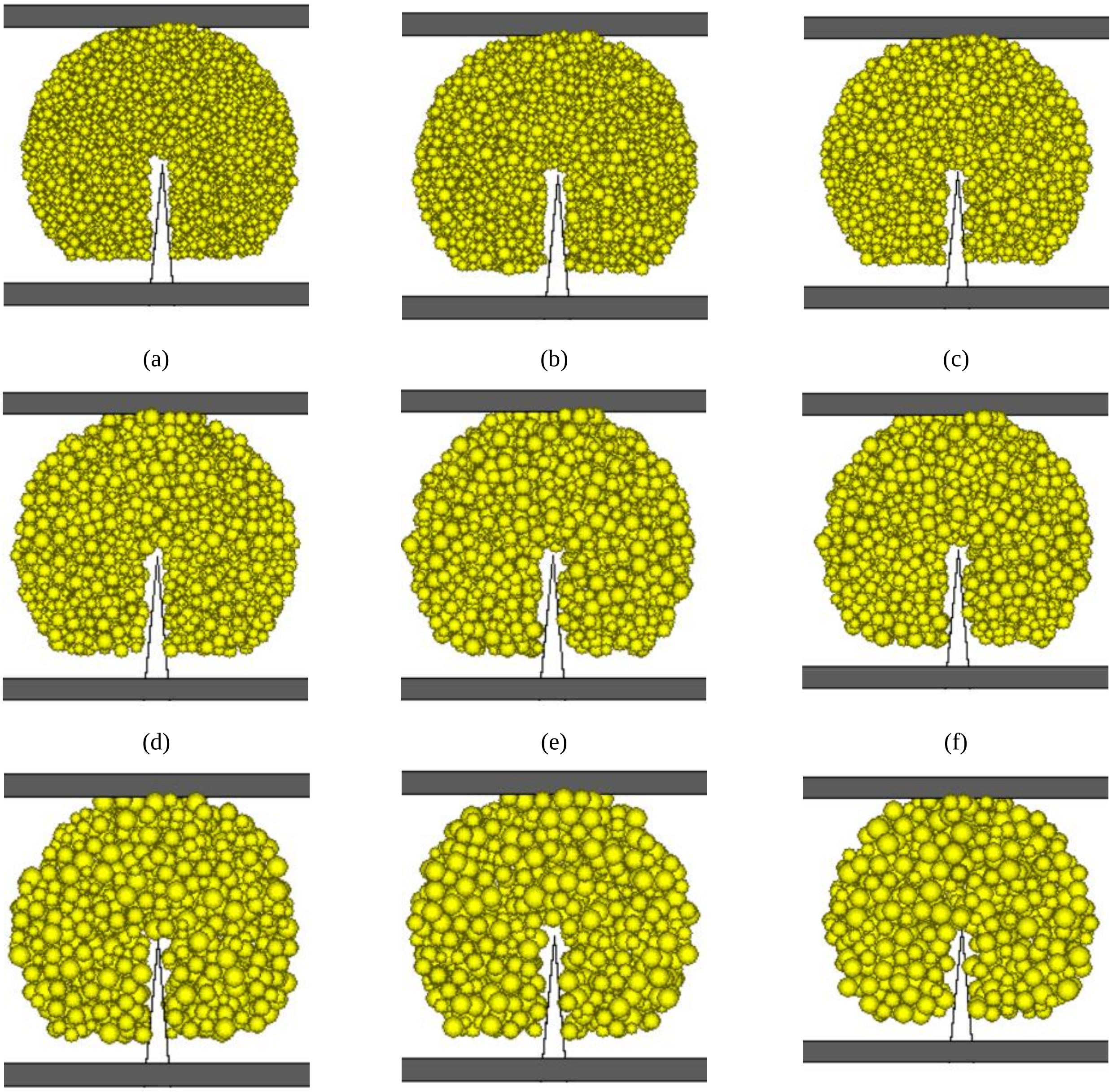

(a) (b) (c) (d) (e) (f) (g) (h) (i)

Continued-

balls, 38495 balls, 22383 balls, 18273 balls, 11104 balls, 8157 balls, 6029 balls, 4834 balls, 3838 balls, 3097 balls, 2535 balls, 2102 balls, 1761 balls, 1491 balls, 1273 balls, 1096 balls, 950 balls and 829 balls, respectively. Black line and red line shows the tensile crack and shear crack; respectively. failure pattern is constant by increasing the ball diameter. Tensile cracks are dominant mode of failure.
These crack initiates from notch tip, propagate parallel to loading axis and coalescence with upper model boundary. Its to be note that number of cracks increase by decreasing the ball diameter.

3.2The effect of particle size on the tensile fracture toughness

Tensile fracture toughness was measured by using Eq. (1). Fig. 6 shows the effect of particle size on the tensile fracture toughness. The results shows that tensile fracture toughness was decreased with increasing the particle size.

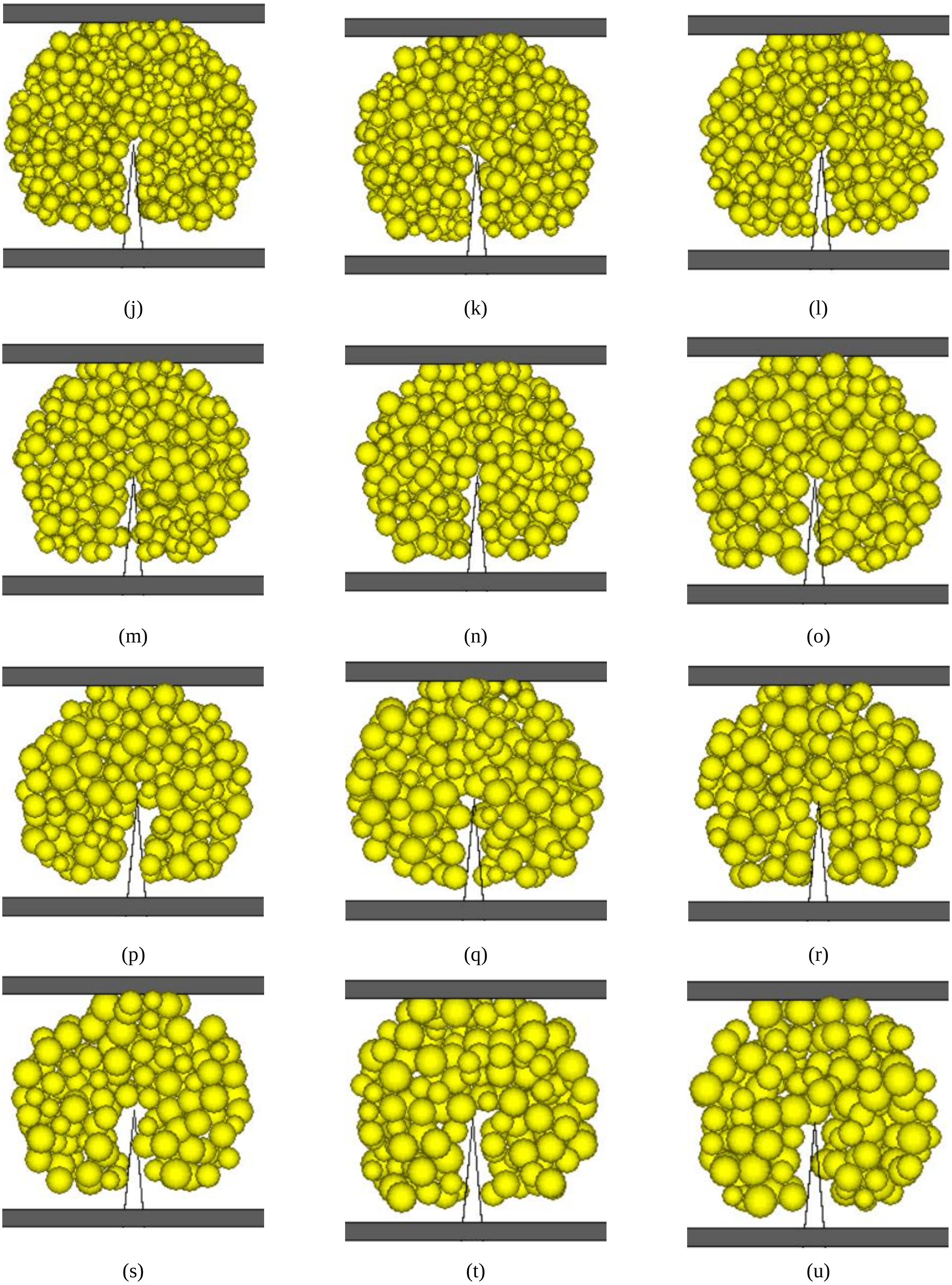

Fig. 4 Edge notched disk with different ball radius of, (a) 0.95 mm, (b) 1.05 mm, (c) 1.15 mm, (d) 1.25 mm, (e) 1.35 mm, (f)1.45 mm, (g) 1.55 mm, (h) 1.65 mm, (i) 1.75 mm, Continued; edge notched disk with different ball radius of, (j) 1.85 mm, (k) 1.95 mm, (l) 2.05 mm, (m) 2.15 mm, (n) 2.25 mm, (o) 2.35 mm, (p) 2.45 mm, (q) 2.55, (r) 2.65 mm, Continued; edge notched disk with different ball radius of, (s) 2.75 mm, (t) 2.85 mm and (u) 2.95 mm

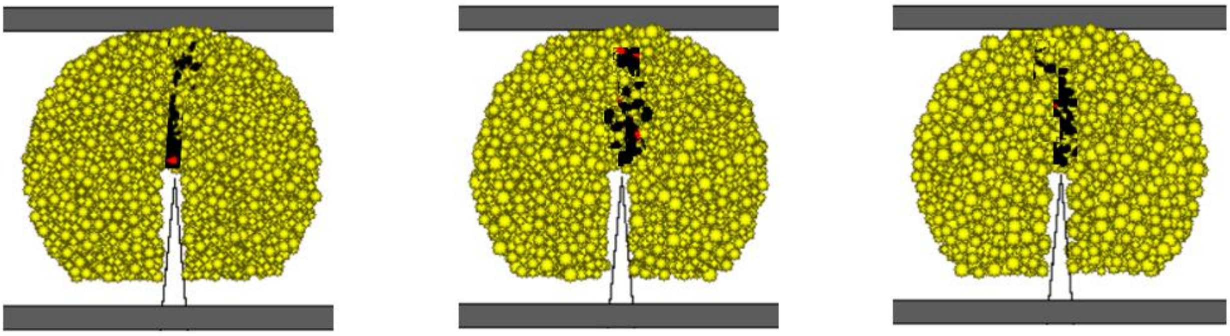

(a) (b) (c)

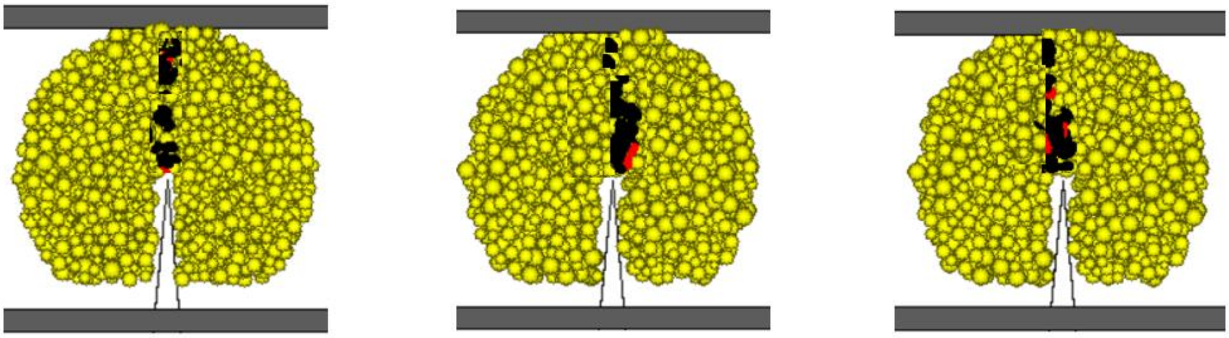

(d) (e) (f)

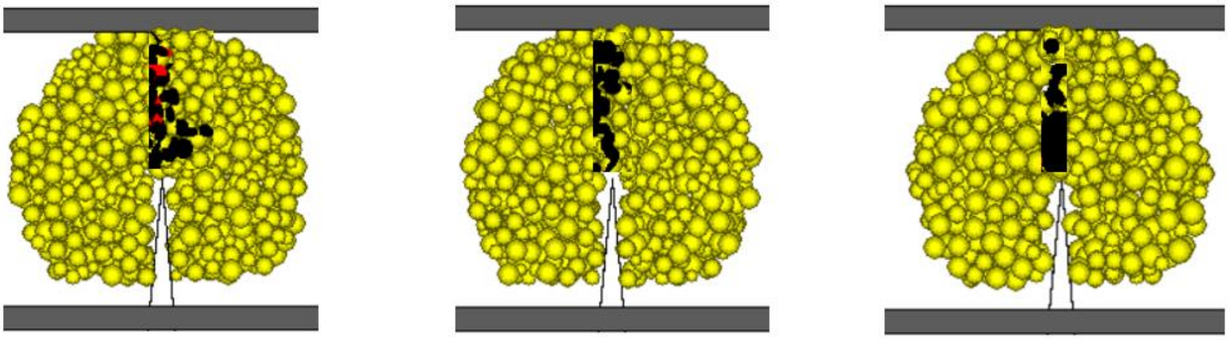

(g) (h) (i)

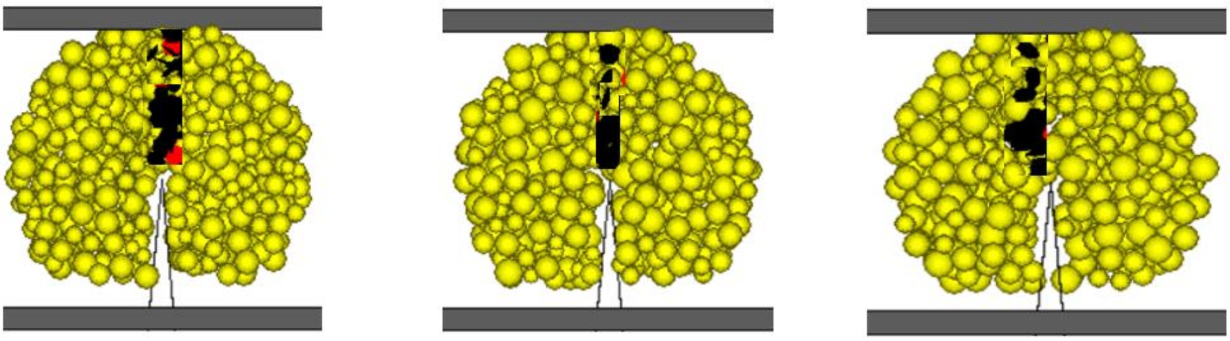

(j) (k) (l)

Continued-

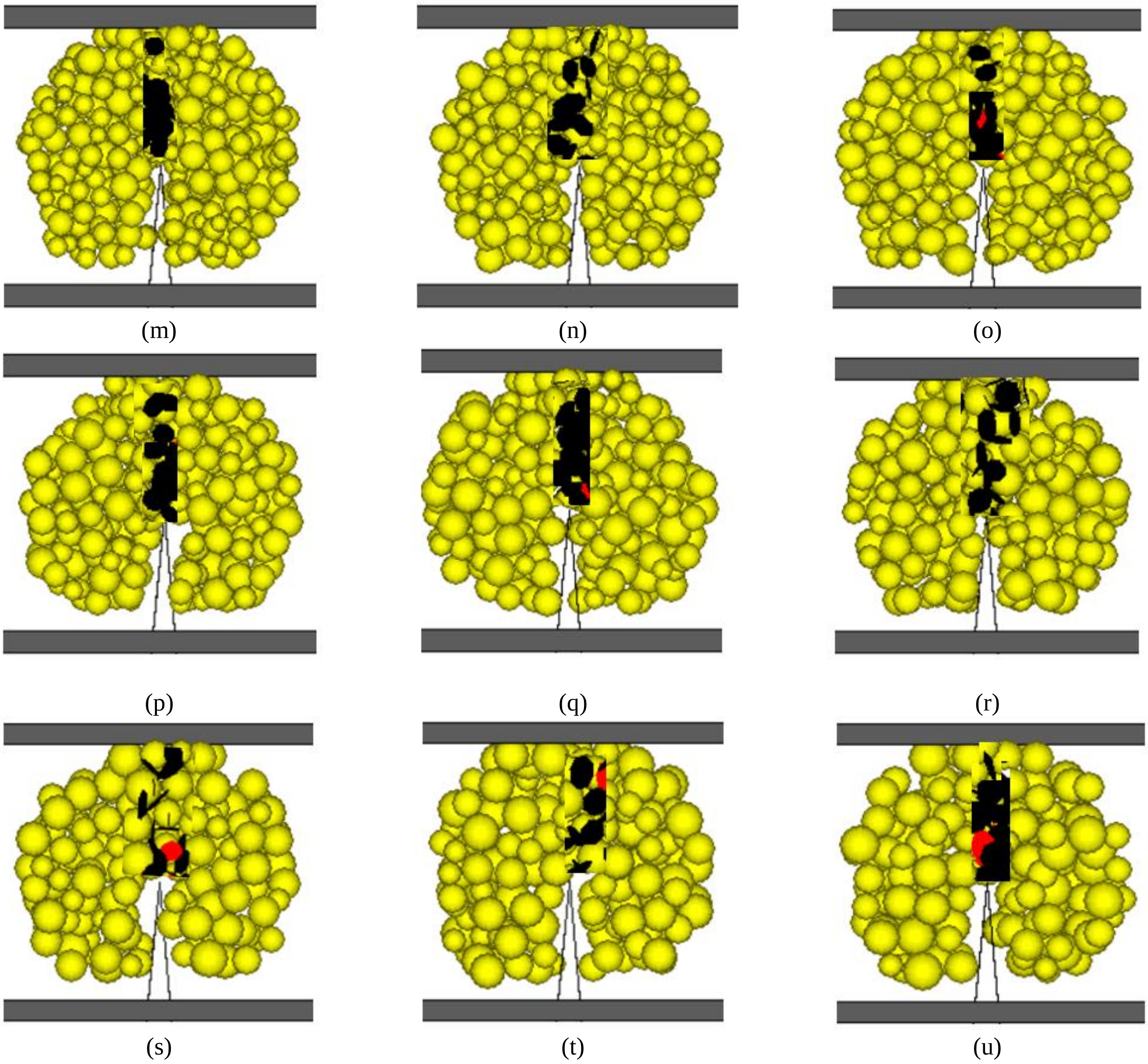

Fig. 5 Failure pattern in edge notched disk with different ball radius of, (a) 0.95 mm, (b) 1.05 mm, (c) 1.15 mm, (d) 1.25 mm, (e) 1.35 mm, (f) 1.45 mm, (g) 1.55 mm, (h) 1.65 mm, (i) 1.75 mm, Continued; failure pattern in edge notched disk with different ball radius of, (j) 1.85 mm, (k) 1.95 mm, (l) 2.05 mm, (m) 2.15 mm, (n) 2.25 mm, (o) 2.35 mm, (p) 2.45 mm, (q) 2.55 and (r)2.65 mm

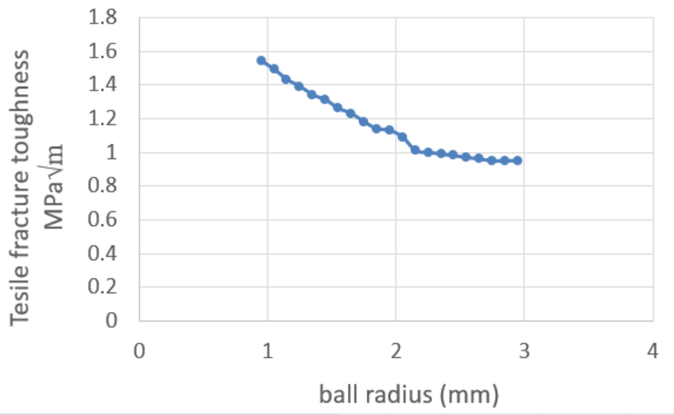

Fig. 6 The effect of particle size on the tensile fracture toughness

4. Conclusions

In this work the effect of particle size on the failure pattern and tensile fracture toughness in edge notched disk has been investigated using PFC3D. Firstly calibration of pfc2d was performed using Brazilian tensile strength. Secondly END test models consisting different particle size was simulated numerically. The results show that:

- Failure pattern is constant by increasing the ball diameter.
- Tensile cracks are dominant mode of failure.
- These crack initiates from notch tip, propagate parallel to loading axis and coalescence with upper model boundary.
- Number of cracks increase by decreasing the ball diameter.
- Tensile fracture toughness was decreased with increasing the particle size.

References

Akbas, S. (2016), "Analytical solutions for static bending of edge cracked micro beams", *Struct. Eng. Mech*., **59**(3), 66-78.

Aliha, M.R., Bahmani, A. and Akhondi, S. (2015a), "Determination of mode III fracture toughness for different materials using a new designed test configuration", *Mater. Design*, **86**, 863-871.

Aliha, M.R., Bahmani, A. and Akhondi, S. (2015b), "Numerical analysis of a new mixed mode I/III fracture test specimen", *Eng. Fract. Mech*., **134**, 95-110.

Amrollahi, H., Baghbanan, A. and Hashemolhosseini, H. (2011), "Measuring fracture toughness of crystalline marbles under modes I and II and mixed mode I-II loading conditions using CCNBD and HCCD specimens", *J. Rock Mech. Min. Sci*., **48**(7), 1123-1134.

Atkinson, B.K. (1987), Fracture Mechanics of Rock, Academic Press, London, U.K.

Atkinson, C., Smelser, R.E. and Sanchez, J. (1982), "Combined mode fracture via the cracked Brazilian disc test", *J. Fracture*, **18**(4), 279-291.

Ayatollahi, M.R. and Alborzi, M.J. (2013), "Rock fracture toughness testing using SCB specimen", *Proceedings of the 13th International Conference on Fracture*, Beijing, China, June.

Banks-Sills, L. and Bortman, Y. (1986), "A mixed mode fracture specimen: Analysis and testing", *J. Fracture*, **30**(3), 181-201.

Barker, L.M. (1977), "A simplified method for measuring plane strain fracture toughness", *Eng. Fract. Mech*., **9**(2), 361-369.

Buchholz, F.G., Pirro, P.J.M., Richard, H.A. and Dreyer, K.H. (1987), "Numerical and experimental mixed-mode analysis of a compact tension-shear-specimen", *Proceedings of the 4th International Conference Numerical Methods in Fracture Mechanics*, Pineridge Press.

Chang, S.H., Lee, C.I. and Jeon, S. (2002), "Measurement of rock fracture toughness under modes I and II and mixed-mode conditions by using disc- type specimen", *Eng. Geol*., **66**(1), 997.

Chong, K.P. and Kuruppu, M.D. (1984), "New specimen for fracture toughness determination for rock and other materials", *J. Fracture*, **26**(2), 59-62.

Chong, K.P., Kuruppu, M.D. and Kuszmaul, J.S. (1987), "Fracture toughness determination of layered materials", *Eng. Fract. Mech*., **28**(1), 43-54.

Cundall, P.A. and Strack, O. (1979), "A discrete element model for granular assemblies", *Geotech*., **29**(1), 47-65.

Dai, F., Chen, R., Iqbal, M.J. and Xia, K. (2010), "Dynamic cracked chevron notched Brazilian disc method for measuring rock fracture parameters", *J. Rock Mech. Min. Sci*., **47**(4), 606613.

Fan, Y., Zhu, Z., Kang, J. and Fu, Y. (2016), "The mutual effects between two unequal collinear cracks under compression", *Math. Mech. Solids*, **22**,1205-1218

Fayed, A.S. (2017), "Numerical analysis of mixed mode I/II stress intensity factors of edge slant cracked plates", *Eng. Sol. Mech*., **5**(1), 61-70.

Gerges, N., Issa, C. and Fawaz, S. (2015), "Effect of construction joints on the splitting tensile strength of concrete", *Case Studies Constr. Mater*., **3**, 83-91.

Hadei1, R. and Kemeny, J. (2016), "New development to measure mode I fracture toughness in rock", *Period. Polytech. Civil Eng*., **61**(1), 51.

Haeri, H. (2015d), "Propagation mechanism of neighboring cracks in rock-like cylindrical specimens under uniaxial compression", *J. Min. Sci*., **51**(3), 487-496.

Haeri, H. (2015e), "Influence of the inclined edge notches on the shear-fracture behavior in edge-notched beam specimens", *Comput. Concrete*, **16**(4), 605-623.

Haeri, H. (2015f), "Experimental crack analysis of rock-like CSCBD specimens using a higher order DDM", *Comput. Concrete*, **16**(6), 881-896.

Haeri, H. and Sarfarazi, V. (2016a), "The effect of micro pore on the characteristics of crack tip plastic zone in concrete", *Comput. Concrete*, **17**(1), 107-112.

Haeri, H., Khaloo, K. and Marji, M.F. (2015b), "Experimental and numerical analysis of Brazilian discs with multiple parallel cracks", *Arab. J. Geosci*., **8**(8), 5897-5908

Haeri, H., Marji, M.F. and Shahriar, K. (2015a), "Simulating the effect of disc erosion in TBM disc cutters by a semi-infinite DDM", *Arab. J. Geosci*., **8**(6), 3915-3927.

Haeri, H., Sarfarazi, V. and Lazemi, H. (2016b), "Experimental study of shear behavior of planar non-persistent joint", *Comput. Concrete*, **17**(5), 639-653.

Haeri, H., Shahriar, K., Marji, M.F. and Moarefvand, P. (2014), "Investigating the fracturing process of rock-like Brazilian discs containing three parallel cracks under compressive line loading", *Strut. Mater*., **46**(3), 133-148.

Haeri, H., Shahriar, K., Marji, M.F. and Moarefvand, P. (2015c), "The HDD analysis of micro cracks initiation, propagation and coalescence in brittle substances", *Arab. J. Geosci*., **8**, 28412852.

He, M.Y., Cao, H.C. and Evans, A.G. (1990), "Mixed-mode fracture: The four point shear specimen", *Acta Metal Mater*., **38**(5), 839-846.

Huang, J. and Wang, S. (1985), "An experimental investigation concerning the comprehensive fracture toughness of some brittle rocks", *J. Rock Mech. Min. Sci. Geomech. Abstr*., **22**(2), 99-104.

Isida, M., Imai, R. and Tsuru, H. (1979), "Symmetric plane problems of arbitrarily shaped plates with an edge crack", *T. Jap. Soc. Mech. Eng*., **45**(395), 743-749.

ISRM (2007), The Complete ISRM Suggested Methods for Rock Characterization Testing and Monitoring: 1974-2006, International Society for Rock Mechanics, Kozan Ofset, Ankara, Turkey.

Itasca PFC2D (1999), Particle Flow Code in 2 Dimensions, Theory and Background, Itasca Consulting Group, Minneapolis, U.S.A.

Karfakis, M.G. and Akram, M. (1993), "Effects of chemical solutions on rockm fracturing", *J. Rock Mech. Min. Sci. Geomech. Abstr*., **30**(7), 1253-1259.

Kataoka, M. and Obara, Y. (2013), "Estimation of fracture toughness of different kinds of rocks under water vapor pressure by SCB test", *J. MMIJ*, **129**, 425-432.

Kataoka, M., Hashimoto, A., Sato, A. and Obara, Y. (2012), "Fracture toughness of anisotropic rocks by semi-circular bend (SCB) test under water vapor pressure", *Proceedings of the 7th ARMS*, Seoul, Korea, October.

Kataoka, M., Obara, Y. and Kuruppu, M. (2011), "Estimation of fracture toughness of anisotropic rocks by SCB test and visualization of fracture by means of X-ray CT", *Proceedings of the 12th ISRM International Congress*, Beijing, China, October.

Kequan, Y.U. and Zhoudao, L.U. (2015), "Influence of softening curves on the residual fracture toughness of post-fire normal-strength mortar", *Comput. Mortar*, **15**(2), 102-111.

Kequan, Y.U. and Zhoudao, L.U. (2015), "Influence of softening curves on the residual fracture toughness of post-fire normalstrength concrete", *Comput. Concrete*, **15**(2), 102-111.

Khan, K. and Al-Shayea, N.A. (2000), "Effect of specimen geometry and testing method on mixed I-II fracture toughness of a limestone rock from Saudi Arabia", *Rock Mech. Rock Eng*., **33**(3), 179-206.

Khodayar, A. and Nejati, H.R. (2018), "Effect of thermal-induced microcracks on the failure mechanism of rock specimens", *Comput. Concrete*, **22**(1), 93-100

Kuruppu, M.D., Obara, Y., Ayatollahi, M.R., Chong, K.P. and Funatsu, T. (2014), "ISRM-suggested method for determining the mode I static fracture toughness using semi-circular bend specimen", *Rock Mech. Rock Eng*., **47**, 267-274.

Lancaster, I.M., Khalid, H.A. and Kougioumtzoglou, I.A. (2013), "Extended FEM modelling of crack propagation using the semi-circular bending test", *Constr. Build. Mater*., **48**, 270-277

Lee, S. and Chang, Y. (2015), "Evaluation of RPV according to alternative fracture toughness requirements", *Struct. Eng. Mech*., **53**(6), 1271-1286.

Lee, S. and Chang, Y. (2015), "Evaluation of RPV according to alternative fracture toughness requirements", *Struct. Eng. Mech*., **53**(6), 1271-1286.

Li, S., Wang, H., Li, Y., Li, Q., Zhang, B. and Zhu, H. (2016), "A new mini-grating absolute displacement measuring system for static and dynamic geomechanical model tests", *Measurement*, **82**, 421-431.

Li, Y., Zhou, H., Zhu, W., Li, S. and Liu, J. (2015), "Numerical study on crack propagation in brittle jointed rock mass influenced by fracture water pressure", *Materials*, **8**(6), 3364-3376.

Lim, I.L., Johnston, I.W. and Choi, S.K. (1993), "Stress intensity factors for semi-circular specimens under three-point bending", *Eng. Fract. Mech*., 44(3), 363-382.

Lim, I.L., Johnston, I.W., Choi, S.K. and Boland, J.N. (1994), "Fracture testing of a soft rock with semi-circular specimens under three-point loading, part 1-mode I", *J. Rock Mech. Min. Sci*., **31**(3), 185-197.

Liu, X., Nie, Z., Wu, S. and Wang, C. (2015), "Self-monitoring application of conductive asphalt concrete under indirect tensile deformation", *Case Studies Constr. Mater*., **3**, 70-77.

Lu, F.Y., Lin, Y.L., Wang, X.Y., Lu, L. and Chen, R. (2015), "A theoretical analysis about the influence of interfacial friction in SHPB tests", *Int. J. Impact. Eng*., **79**, 95-101.

Maccagno, T.M. and Knott, J.F. (1989), "The fracture behaviour of PMMA in mixed modes I and II", *Eng. Fract. Mech*., **34**(1), 65-86.

Mahajan, R.V. and Ravi-Chandar, K. (1989), "An experimental investigation of mixed-mode fracture", *J. Fracture*, **41**(4), 235252.

Mobasher, B., Bakhshi, M. and Barsby, C. (2014), "Backcalculation of residual tensile strength of regular and high performance fibre reinforced concrete from flexural tests", *Constr. Build. Mater*., **70**, 243-253.

Mohammad, A. (2016), "Statistical flexural toughness modeling of ultra high performance concrete using response surface method", *Comput. Concrete*, **17**(4), 33-39.

Molenar, A.A.A., Scarpas, A., Liu, X. and Erkens, S.M.J.G. (2002), "Semi-circular bending test: Simple but useful?", *J. Assoc. Asph. Pav. Technol*., **71**, 794-815.

Najigivi, A., Nazerigivi, A. and Nejati, H.R. (2017), "Contribution of steel fiber as reinforcement to the properties of cement-based concrete: a review", *Comput. Concrete*, **20**(2), 155-164.

Nazerigivi, A., Nejati, H.R., Ghazvinian, A. and Najigivi, A. (2017), "Influence of nano-silica on the failure mechanism of concrete specimens", *Comput. Concrete*, **19**(4), 429-434.

Noel, M. and Soudki, K. (2014), "Estimation of the crack width and deformation of FRP-reinforced concrete flexural members with and without transverse shear reinforcement", *Eng. Struct.*, **59**, 393-398.

Obara, Y., Kuruppu, M. and Kataoka, M. (2010), "Determination of fracture toughness of anisotropic rocks under water vapour pressure by semi-circular bend test", *Proceedings of the Mine Planning and Equipment Selection*, Victoria, Australia.

Obara, Y., Sasaki, K. and Yoshinaga, T. (2007), "Estimation of fracture toughness of rocks under water vapour pressure by semi-circular bend (SCB) test", *J. MMIJ*, **123**(4-5), 145-151.

Obara, Y., Yoshinaga, T. and Hirata, A. (2009), "Fracture toughness in mode I and II of rock under water vapour pressure", *Proceedings of the ISRM Regional Symposium EUROCK*, Cavtat, Italy.

Oliveira, H.L., and Leonel, E.D. (2014), "An alternative BEM formulation, based on dipoles of stresses and tangent operator technique, applied to cohesive crack growth modeling", *Eng. Anal. Bound. Elem*., **41**, 74-82.

Ouchterlony, F. (1980), A New Core Specimen for the Fracture Toughness Testing of Rock, Swedish Detonic Research Foundation Report, Stockholm, Sweden.

Ouchterlony, F. (1981), Extension of the Compliance and Stress Intensity Formulas for the Single Edge Crack Round Bar in Bending, ASTM STP 745.

Ouchterlony, F. (1986), "Suggested methods for determining the fracture toughness of rock", J. *Rock Mech. Min. Sci. Geomech. Abstr*., **25**(1), 71-96.

Pan, B., Gao, Y. and Zhong, Y, (2014), "Theoretical analysis of overlay resisting crack propagation in old cement mortar pavement", *Struct. Eng. Mech*., **52**(4) 167-181.,

Potyondy, D.O. and Cundall, P.A. (2004), "A bonded-particle model for rock", *J. Rock Mech. Min. Sci*., **41**(8), 1329-1364.

Potyondy, D.O., Cundall, P.A. and Lee, C. (1996), "Modeling of rock using bonded assemblies of circular particles", *Proceedings of 2nd North American Rock Mechanics Symposium*, *Montreal*, Vancouver.

Rajabi, M., Soltani, N. and Eshraghi, I. (2016), "Effects of temperature dependent material properties on mixed mode crack tip parameters of functionally graded materials", *Struct. Eng. Mech*., **58**(2), 144-156.

Ramadoss, P. and Nagamani, K. (2013), "Stress-strain behavior and toughness of high-performance steel fiber reinforced mortar in compression", *Comput. Mortar*, **11**(2), 55-65.

Sardemir, M., (2016), "Empirical modeling of flexural and splitting tensile strengths of concrete containing fly ash by GEP", *Comput. Concrete*, **17**(4), 489-498.

Sarfarazi, V. and Haeri, H. (2016), "Effect of number and configuration of bridges on shear properties of sliding surface", *J. Min. Sci*., **52**(2), 245-257.

Sarfarazi, V. and Haeri, H. (2016c), "A review of experimental and numerical investigations about crack propagation", *Comput. Concrete*, **18**(2), 235-266.

Sarfarazi, V. and Shubert, W. (2016b), "Numerical simulation of tensile failure of concrete in direct, flexural, double punch tensile and ring tests", *Period. Polyech. Civil Eng*., **2**, 1-8.

Sarfarazi, V., Faridi, H.R., Haeri, H. and Schubert, W. (2016c), "A new approach for measurement of anisotropic tensile strength of concrete", *Adv. Concrete Constr*., **3**(4), 269-284.

Sarfarazi, V., Ghazvinian, A., Schubert, W., Blumel, M. and Nejati, H.R. (2014), "Numerical simulation of the process of fracture of echelon rock joints", *Rock Mech. Rock Eng*., **47**(4), 1355-1371.

Sarfarazi, V., Haeri, H. and Khaloo, A. (2016a), "The effect of non-persistent joints on sliding direction of rock slopes", *Comput. Concrete*, **17**(6), 723-737.

Sato, K. (2006), "Fracture toughness evaluation based on tensionsoftening model and its application to hydraulic fracturing", *Pure Appl. Geophys*., **163**(5), 1073-1089.

Shiryaev, A.M. and Kotkis, A.M. (1982), "Methods for determining fracture toughness of brittle porous materials", *Industr. Labor*., **48**(9), 917-918.

Shuraim, A.B., Aslam, F., Hussain, R. and Alhozaimy, A. (2016), "Analysis of punching shear in high strength RC panels–experiments, comparison with codes and FEM results", *Comput. Concrete*, **17**(6), 739-760.

Silva, R.V., Brito, J. and Dhir, R.K. (2015), "Tensil strength behaviour of recycled aggregate concrete", *Constr. Build. Mater*., **83**, 108-118.

Singh, R.N. and Sun, G.X. (1990), "A numerical and experimental investigation for determining fracture toughness of welsh limestone", *Min. Sci. Technol*., **10**(1), 61-70.

Suresh, S. and Shih, C.F., Morrone, A. and O'Dowd, N.P. (1990), "Mixed-mode fracture toughness of ceramic materials", *J. Am. Ceram. Soc*., **73**(5), 1257-1267.

Tiang, Y., Shi, S., Jia, K. and Hu, S. (2015), "Mechanical and dynamic properties of high strength concrete modified with lightweight aggregates presaturated polymer emulsion", *Constr. Build. Mater*., **93**, 1151-1156,

Tutluoglu, L. and Keles, C. (2011), "Mode I fracture toughness determination with straight notched disk bending method", *J. Rock Mech. Min. Sci*., **48**(8), 1248-1261.

Wan Ibrahim, M.H., Hamzah, A.F., Jamaluddin, N., Ramadhansyah, P.J. and Fadzil, A.M. (2015), "Split tensile strength on self-compacting concrete containing coal bottom ash", *Procedia - Social and Behavioral Sciences*, **198**, 2280-2289.

Wang, Q.Z., Feng, F., Ni ,M. and Gou, X.P. (2011), "Measurement of mode I and mode II rock dynamic fracture toughness with cracked straight through flattened Brazilian disc impacted by split Hopkinson pressure bar", *Eng. Fract. Mech*., **78**(12), 2455-2469

Wang, X., Zhu, Z., Wang, M., Ying, P., Zhou, L. and Dong, Y. (2017), "Study of rock dynamic fracture toughness by using VB-SCSC specimens under medium-low speed impacts", *Eng. Fract. Mech*., **181**; 52-64.

Wu, Z.J., Ngai, L. and Wong, Y. (2014), "Investigating the effects of micro-defects on the dynamic properties of rock using Numerical Manifold method", *Constr. Build. Mater*., **72**, 72-82.

Yaylac, M. (2016), "The investigation crack problem through numerical analysis", *Struct. Eng. Mech*., **57**(6), 1143-1156.

Zhang, Q.B. and Zhao, J. (2014), "Quasi-static and dynamic fracture behaviour of rock materials: phenomena and mechanisms", *Int. J. Fract*., **189**, 1-32

Zhao, Y., Zhao, G.F. and Jiang, Y. (2013), "Experimental and numerical modelling investigation on fracturing in coal under impact loads", *Int. J. Fract*., **183**(1), 63-80.

Zhou, Y.X., Xia, K., Li, X.B., Li, H.B., Ma, G.W., Zhao, J., Zhou, Z.L. and Dai, F. (2012), "Suggested methods for determining the dynamic strength parameters and mode-I fracture toughness of rock materials", *J. Rock Mech. Min. Sci*., **49**, 105-112.

CC